

Multiple-scattering analysis of the structure of ethylene adsorbed on the Cu(100) surface

J. C. Tang, X. S. Feng, and J. F. Shen

*Physics Department, Zhejiang University, Hangzhou 310 027, China
and China Center of Advanced Science and Technology, P.O. Box 8730, Beijing 100 080, China*

T. Fujikawa and T. Okazawa

Faculty of Engineering, Yokohama National University, Yokohama 240, Japan

(Received 11 February 1991)

The carbon *K*-shell near-edge x-ray-absorption fine-structure (NEXAFS) spectra of gas-phase ethylene molecules and ethylene adsorbed on the Cu(100) surface have been calculated by the multiple-scattering cluster method. The calculated result shows the existence of the C-H scattering resonance in carbon *K*-shell NEXAFS spectra of the adsorbed ethylene molecules. By a comparison between the theoretical results and the experimental spectra, we have found that the C—C bond midpoint occupies a fourfold hollow site 1.3 Å above the Cu surface with the C—C axis being parallel to the [001] or [010] direction. The bond lengths of C—C and Cu—C are equal to 1.46 ± 0.04 and 1.90 ± 0.03 Å, respectively, and the H—C—H bond angle equals $130 \pm 5^\circ$. These results are in agreement with those of Fourier-transform analysis of the surface extended x-ray-absorption fine structure.

I. INTRODUCTION

In the recent years, the near-edge x-ray-absorption fine-structure (NEXAFS) technique has been extensively used for the structure investigation of chemisorbed molecules. NEXAFS studies can enhance our knowledge of the microscopic characteristics of chemisorption, such as the orientation of the molecule adsorbed on the substrate, the bond length between the adsorbate and the substrate atoms, the coordination to the substrate atoms, and the change of intramolecular bond length in the chemisorption process.

NEXAFS and surface extended x-ray-absorption fine-structure (SEXAFS) spectra of ethylene (C_2H_4) adsorbed on a metal surface have been measured using synchrotron radiation in recent years.^{1,2} The experimental results of NEXAFS indicate that the C_2H_4 molecule lies flat on the Cu and Ag surface; furthermore, Fourier-transform analysis of SEXAFS demonstrates a possible structure model of C_2H_4 -Cu(100). However, there are no theoretical calculations to support the above result.

It is interesting that an angular dependence of the C-H scattering resonance exists in the carbon *K*-shell excitation spectra of the chemisorbed hydrocarbon system. This opens the way for NEXAFS studies of hydrogenation and dehydrogenation reactions.³

In this paper we present theoretical studies of carbon *K*-shell NEXAFS spectra of gas-phase ethylene molecules and C_2H_4 adsorbed on Cu(100). We have considered all multiple-scattering effects in a cluster which comprises one adsorbed molecule and several neighboring atoms in the substrate. This cluster simulates the adsorbate-substrate system, therefore this is a multiple-scattering cluster (MSC) method for NEXAFS. It is different from the self-consistent-field- $X\alpha$ -scattered-wave (SCF- $X\alpha$ -SW) calculation of NEXAFS.⁴ However, Durham, Pen-

dry, and Hodges⁵ have considered multiple-scattering effects in NEXAFS [it is also called x-ray absorption near-edge structure^{5,6} (XANES)]; their XANES code is based upon a cluster method and includes full multiple-scattering contributions. The cluster is divided into concentric shells of atoms centered around the absorbing atom. The multiple-scattering equations are solved first within each shell and then between the shells themselves and the central atom.

In our MSC method, the summations of all scattering events are taken over all of the individual atoms rather than over the atomic shells. This summation can be made directly if the total number of atoms in the cluster is not too large. For example, in the adsorbate-substrate system we may select 20 or fewer atoms without requiring excessive computer time.

II. DESCRIPTION OF MSC METHOD OF NEXAFS

NEXAFS and core-level photoelectron diffraction have the same physical origin, i.e., the x ray excites the core-level electrons and the excited photoelectrons are scattered by neighboring atoms which surround the excited one. It is found that the NEXAFS process is dominated by the electric dipole transition to σ^* and π^* final states.⁷ In the SEXAFS region the single-scattering calculation works well, but in the NEXAFS region it is necessary to consider multiple-scattering effects.⁸

According to the dynamic theory of photoelectron diffraction the wave function of a photoelectron located at \mathbf{R} can be written as^{9,10}

$$\Psi(\mathbf{R}) = \int G(\mathbf{R}, \mathbf{r}) H_{\text{int}}(\mathbf{r}) \psi_i(\mathbf{r}) d\tau, \quad (1)$$

where H_{int} is the interaction between the photon and solids, and ψ_i is the initial wave function of the electron. The Green's function $G(\mathbf{R}, \mathbf{r})$ of the entire system can be

calculated by the propagator of the free electron (G_0) and the atomic t matrix,

$$G = G_0 + G_0 t_\alpha G_0 + \sum_{\beta \neq \alpha} G_0 t_\beta G_0 + \sum_{\nu \neq \beta} \sum_{\beta \neq \alpha} G_0 t_\nu G_0 t_\beta G_0 + \dots \quad (2)$$

Then $\Psi(\mathbf{R})$ can be separated into two parts,

$$\Psi(\mathbf{R}) = \psi_D(\mathbf{R}) + \psi_S(\mathbf{R}), \quad (3)$$

where ψ_D represents direct emission of the photoelectron from the central atom, which does not include the scattering effects of the photoelectron between the excited atom and its neighborhood. The latter are given by

$$\psi_D(\mathbf{R}) = \int (G_0 + \int G_0 t_\alpha G_0 d\tau') H_{\text{int}} \psi_i(\mathbf{r}) d\tau. \quad (4)$$

It can be shown that the asymptotic form of ψ_D is

$$\psi_1(\mathbf{R}) = \sum_{\beta \neq \alpha} \int \int G_0(\mathbf{R}, \mathbf{r}_1) t_\beta(\mathbf{r}_1, \mathbf{r}) \psi_D(\mathbf{r}) d\mathbf{r} d\mathbf{r}_1, \quad (8)$$

$$\psi_2(\mathbf{R}) = \sum_{\nu \neq \beta} \sum_{\beta \neq \alpha} \int \int \int \int G_0(\mathbf{R}, \mathbf{r}_2) t_\nu(\mathbf{r}_2, \mathbf{r}_1) G_0(\mathbf{r}_1, \mathbf{r}') t_\beta(\mathbf{r}', \mathbf{r}) \Psi_D(\mathbf{r}) d\mathbf{r} d\mathbf{r}_1 d\mathbf{r}_2 d\mathbf{r}'. \quad (9)$$

It is well known that ψ_1 and ψ_2 describe the single- and double-scattering events, respectively, their asymptotic form being as follows:

$$\psi_1(\mathbf{R}) \sim \frac{2m}{\hbar^2} \frac{e^{ikR}}{R} \sum_{\beta \neq \alpha} e^{-ik \cdot \mathbf{R}_\beta} \sum_{L, L'} Y_{L'}^*(\mathbf{R}) t_{L'}^\beta G_{L'L}(\mathbf{R}_\beta - \mathbf{R}_\alpha) M_L^\alpha \quad \text{as } R \rightarrow \infty, \quad (10)$$

in which $t_{L'}^\beta$ is related to the phase shift $\delta_{L'}^\beta$ by

$$t_{L'}^\beta = -\frac{e^{2i\delta_{L'}^\beta} - 1}{2ik}, \quad (11)$$

and

$$G_{L'L}(\mathbf{R}_\beta - \mathbf{R}_\alpha) = -\frac{8\pi ikm}{\hbar^2} \sum_{L''} i^{L''} a(L, L', L'') h_{L''}^{(1)}(k|\mathbf{R}_\beta - \mathbf{R}_\alpha|) Y_{L''}(\mathbf{R}_\beta - \mathbf{R}_\alpha), \quad (12)$$

$$a(L, L', L'') = \int Y_L(\mathbf{k}) Y_{L'}^*(\mathbf{k}) Y_{L''}(\mathbf{k}) d\Omega_K. \quad (13)$$

In Eq. (12), $h_{L''}^{(1)}$ is a spherical Hankel function of the first kind. In the same way, we have

$$\psi_2(\mathbf{R}) \sim \frac{2m}{\hbar^2} \frac{e^{ikR}}{R} \sum_{\nu \neq \beta} \sum_{\beta \neq \alpha} e^{-ik \cdot \mathbf{R}_\nu} \sum_L \sum_{L'} \sum_{L''} Y_{L''}^*(\mathbf{R}) t_{L''}^\nu G_{L''L'}(\mathbf{R}_\nu - \mathbf{R}_\beta) t_{L'}^\beta G_{L'L}(\mathbf{R}_\beta - \mathbf{R}_\alpha) M_L^\alpha \quad \text{as } R \rightarrow \infty. \quad (14)$$

Therefore the asymptotic behavior of the scattering wave can be summarized as follows:¹¹

$$\psi_S(\mathbf{R}) \sim \frac{2m}{\hbar^2} \frac{e^{ikr}}{R} \sum_\nu e^{-ik \cdot \mathbf{R}_\nu} \sum_{L_1} Y_{L_1}^*(\mathbf{R}) [\hat{T}(1 - \hat{T})^{-1}]_{\alpha L_1}^{\nu L_1} M_L^\alpha \quad \text{as } R \rightarrow \infty, \quad (15)$$

where the matrix \hat{T} is given by

$$(\hat{T})_{\alpha L_1}^{\nu L_1} = \begin{cases} 0, & \nu = \alpha \\ t_{L_1}^\nu G_{L_1 L}(\mathbf{R}_\nu - \mathbf{R}_\alpha), & \nu \neq \alpha \end{cases}. \quad (16)$$

The differential cross section of the NEXAFS is proportional to the absolute square of the wave function,

$$\sigma(\mathbf{R}) \propto |\psi_D(\mathbf{R}) + \psi_S(\mathbf{R})|^2, \quad (17)$$

$$\psi_D(\mathbf{R}) \sim \frac{2m}{\hbar^2} \frac{e^{ikr}}{R} e^{-ik \cdot \mathbf{R}_\alpha} \sum_L Y_L(\mathbf{R}) M_L^\alpha \quad \text{as } R \rightarrow \infty, \quad (5)$$

in which the excitation matrix element M_L^α is written as

$$M_L^\alpha = -(-i)^l \int e^{i\delta_l^\alpha} R_l^\alpha(\rho) Y_L^*(\rho) H_{\text{int}} \psi_i(\rho) d\rho, \quad (6)$$

where δ_l^α is the L th phase shift of the atom α , and $R_l^\alpha(\rho)$ is the radial wave function of the excited state of the atom α .

In the multiple-scattering regime, the scattering wave is an infinite geometrical series,

$$\psi_S(\mathbf{R}) = \sum_{n=1}^{\infty} \psi_n(\mathbf{R}), \quad (7)$$

in which the first two terms are given by

$$\psi_1(\mathbf{R}) = \sum_{\beta \neq \alpha} \int \int G_0(\mathbf{R}, \mathbf{r}_1) t_\beta(\mathbf{r}_1, \mathbf{r}) \psi_D(\mathbf{r}) d\mathbf{r} d\mathbf{r}_1, \quad (8)$$

$$\psi_2(\mathbf{R}) = \sum_{\nu \neq \beta} \sum_{\beta \neq \alpha} \int \int \int \int G_0(\mathbf{R}, \mathbf{r}_2) t_\nu(\mathbf{r}_2, \mathbf{r}_1) G_0(\mathbf{r}_1, \mathbf{r}') t_\beta(\mathbf{r}', \mathbf{r}) \Psi_D(\mathbf{r}) d\mathbf{r} d\mathbf{r}_1 d\mathbf{r}_2 d\mathbf{r}'. \quad (9)$$

It is well known that ψ_1 and ψ_2 describe the single- and double-scattering events, respectively, their asymptotic form being as follows:

$$\psi_1(\mathbf{R}) \sim \frac{2m}{\hbar^2} \frac{e^{ikR}}{R} \sum_{\beta \neq \alpha} e^{-ik \cdot \mathbf{R}_\beta} \sum_{L, L'} Y_{L'}^*(\mathbf{R}) t_{L'}^\beta G_{L'L}(\mathbf{R}_\beta - \mathbf{R}_\alpha) M_L^\alpha \quad \text{as } R \rightarrow \infty, \quad (10)$$

in which $t_{L'}^\beta$ is related to the phase shift $\delta_{L'}^\beta$ by

$$t_{L'}^\beta = -\frac{e^{2i\delta_{L'}^\beta} - 1}{2ik}, \quad (11)$$

and

$$G_{L'L}(\mathbf{R}_\beta - \mathbf{R}_\alpha) = -\frac{8\pi ikm}{\hbar^2} \sum_{L''} i^{L''} a(L, L', L'') h_{L''}^{(1)}(k|\mathbf{R}_\beta - \mathbf{R}_\alpha|) Y_{L''}(\mathbf{R}_\beta - \mathbf{R}_\alpha), \quad (12)$$

$$a(L, L', L'') = \int Y_L(\mathbf{k}) Y_{L'}^*(\mathbf{k}) Y_{L''}(\mathbf{k}) d\Omega_K. \quad (13)$$

In Eq. (12), $h_{L''}^{(1)}$ is a spherical Hankel function of the first kind. In the same way, we have

$$\psi_2(\mathbf{R}) \sim \frac{2m}{\hbar^2} \frac{e^{ikR}}{R} \sum_{\nu \neq \beta} \sum_{\beta \neq \alpha} e^{-ik \cdot \mathbf{R}_\nu} \sum_L \sum_{L'} \sum_{L''} Y_{L''}^*(\mathbf{R}) t_{L''}^\nu G_{L''L'}(\mathbf{R}_\nu - \mathbf{R}_\beta) t_{L'}^\beta G_{L'L}(\mathbf{R}_\beta - \mathbf{R}_\alpha) M_L^\alpha \quad \text{as } R \rightarrow \infty. \quad (14)$$

Therefore the asymptotic behavior of the scattering wave can be summarized as follows:¹¹

$$\psi_S(\mathbf{R}) \sim \frac{2m}{\hbar^2} \frac{e^{ikr}}{R} \sum_\nu e^{-ik \cdot \mathbf{R}_\nu} \sum_{L_1} Y_{L_1}^*(\mathbf{R}) [\hat{T}(1 - \hat{T})^{-1}]_{\alpha L_1}^{\nu L_1} M_L^\alpha \quad \text{as } R \rightarrow \infty, \quad (15)$$

where the matrix \hat{T} is given by

$$(\hat{T})_{\alpha L_1}^{\nu L_1} = \begin{cases} 0, & \nu = \alpha \\ t_{L_1}^\nu G_{L_1 L}(\mathbf{R}_\nu - \mathbf{R}_\alpha), & \nu \neq \alpha \end{cases}. \quad (16)$$

The differential cross section of the NEXAFS is proportional to the absolute square of the wave function,

$$\sigma(\mathbf{R}) \propto |\psi_D(\mathbf{R}) + \psi_S(\mathbf{R})|^2, \quad (17)$$

and the total cross section is the integral of $\sigma(\mathbf{R})$ over all directions,

$$\sigma = \int \sigma(\mathbf{R}) d\Omega. \quad (18)$$

The modulation function is defined as

$$\chi(k) = \frac{\sigma - \sigma_0}{\sigma_0}, \quad \sigma_0 = \int |\psi_D|^2 d\Omega. \quad (19)$$

This quantity can then be compared with experimental spectra.

For the C_2H_4 -Cu(100) system, we have chosen one ethylene molecule as well as its nearest and next-nearest-neighbor atoms in the substrate to construct a cluster. We have constructed six possible clusters to simulate the adsorption system, calculated the C K -shell NEXAFS spectra for these clusters, and made a comparison between the calculated results and the experimental spectra to determine the correct structure of the system.

Inputs to the calculation of the NEXAFS spectra in terms of the MSC method include the positions of the atoms in the cluster, the incident photon direction, and the phase shifts δ_l . We calculate δ_l by the SCF- $X\alpha$ -SW method, which demonstrates high accuracy in dealing with photoelectron diffraction.¹²

III. RESULTS AND DISCUSSION

A. Analysis of the NEXAFS spectrum of a C_2H_4 molecule

The C K -shell NEXAFS spectrum of a gas-phase ethylene molecule has been measured by Hitchcock and Brion¹³ and Sette, Stohr, and Hitchcock.⁷ We have plotted their experimental spectrum in Fig. 1. According to Ref. 7, the intense peak, labeled "1," was assigned the π^* resonance, and two weaker peaks, labeled "2" and "3," were referred to Rydberg states, and the structures "4" and "5" were assigned the multielectron (shake up) states. Moreover, a σ^* resonance was assigned at ~ 300 eV (photon energy). Recently, Stohr, Sette, and Johnson,¹⁴ suggest that peaks 2 and 3 are due to the carbon hydro-

gen resonance.³ But there is no theoretical analysis to support this suggestion as yet.

We have calculated the C K -edge NEXAFS spectra of the gas-phase ethylene molecule in terms of the MSC method. The calculated C K -edge absorption curves were also plotted in Fig. 1. In our calculations we kept the H—C—H bond angle $\alpha=120^\circ$, but changed C—C and C—H bond lengths (L_{C-C} and L_{C-H}) to optimize the calculated results. Figure 1(a) is the plot of the calculated NEXAFS spectra versus L_{C-C} . There are clearly three resonance structures labeled "A," "B," and "BP" appearing in these curves. It is easy to see that the position of the first peak does not shift with L_{C-C} , but its height varies with L_{C-C} dramatically; this is the character of π^* resonance as discussed for O_2 and Co molecules.¹⁵ So we assign the peak A as a π^* resonance after Ref. 7.

When L_{C-C} equals 1.30 \AA the π^* resonance is very weak but as $L_{C-C}=1.34 \text{ \AA}$, it becomes an intense peak; the height of this resonance then decreases as L_{C-C} increases. The best fit between the theoretical curves and the experimental spectrum appears in the case of $L_{C-C}=1.34 \text{ \AA}$. It is interesting that the π^* resonance disappears when $L_{C-C}=1.46 \text{ \AA}$. It implies that the C—C bond is no longer a double bond for so large a bond length; it becomes a single σ bond.

In order to understand the origin of the second peak (B), we kept $L_{C-C}=1.34 \text{ \AA}$ but changed the C—H bond length from 1.0 to 1.12 \AA ; the calculated curves were plotted in Fig. 1(b). These curves are similar to each other, but the position of peak B shifts towards the low-energy direction when L_{C-H} increases. This fact shows that the peak B is closely related with the C—H bond length; we assigned this peak as a C-H resonance the same as that assigned by Stohr, Sette, and Johnson.¹⁴ Furthermore, the assigned position of the C-H resonance coincides with the midpoint of peaks 2 and 3. We then judge that the C—H bond length equals 1.09 \AA .

We now discuss the third peak in Fig. 1(a). This is a very broad structure (labeled "BP"); its energy region corresponds to that of peaks 4 and 5, as well as that of the σ^* resonance. We notice that the peak position of BP shifts towards lower energies as L_{C-C} increases. This is the character of σ resonance versus the intramolecular bond length, so we assign BP the σ^* resonance after Ref. 7. When $L_{C-C}=1.46 \text{ \AA}$, the σ^* resonance coincides with the C-H resonance; they interfere with each other and become an intense peak. Therefore we found the intramolecular bond lengths of ethylene molecule L_{C-C} and L_{C-H} equal 1.34 and 1.09 \AA , respectively. This result agrees with the experimental data.¹⁶

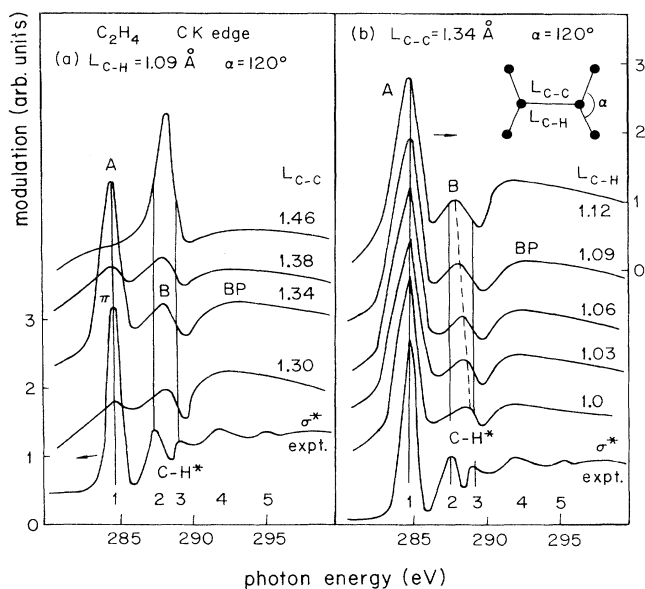


FIG. 1. Calculated C K -shell NEXAFS spectra of a gas-phase ethylene molecule. (a) NEXAFS spectra corresponding to different C—C bond lengths; (b) NEXAFS spectra with different C—H bond lengths. The experimental spectrum is quoted from Ref. 13.

B. Structure determination of C_2H_4 on Cu(100)

1. Determining the intramolecular bond length

In order to understand the process of chemisorption, the most important thing is determining the bond length to the substrate, and the eventual change in the internal structure of the adsorbed molecule. For C_2H_4 -Cu(100),

Arvanitis *et al.*^{1,2} found that the C_2H_4 molecules were lying flat on the surface, and the C—C bond length was elongated due to the interaction between C and Cu substrate. Their experimental C K-shell NEXAFS spectra were plotted in Fig. 2. The experiment was performed with two incident angles: one is 10° , the linearly polarized electric field E almost perpendicular to the surface, and the other is 90° , with E parallel to the surface. For grazing incidence, the sharp feature at 284.6 eV is assigned as a π^* resonance and the energy position is the same as that in the spectrum of gas-phase ethylene molecules. In contrast, the broad feature around 296 eV has maximum intensity for normal incidence and is assigned the σ^* resonance.

We have performed a MSC calculation with an aligned-hollow model (see the inset of Fig. 2). The plane of the polarization vector is perpendicular to the Cu(100) surface with the azimuth along the $\langle 001 \rangle$ direction. We changed the C—C bond length L_{C-C} from 1.42 to 1.54 Å, then calculated the C K-edge absorption spectra. At grazing incidence, the calculated curves are similar to each other, in which there are three peaks labeled I, II, and III. They fit with experiment very well, but we cannot find the intramolecular bond length of adsorbed molecules from this calculation. At normal incidence, the position of peak C shifts towards lower energies as L_{C-C} increases; this is the character of the σ^* resonance. Comparing these curves with the experimental spectrum, we found that the curve corresponding to $L_{C-C} = 1.46$ Å fits with the experimental spectrum well. This C—C bond length is longer than that in gas-phase ethylene molecules; the elongation of L_{C-C} is due to the interaction between C atoms and the Cu substrate. It seems

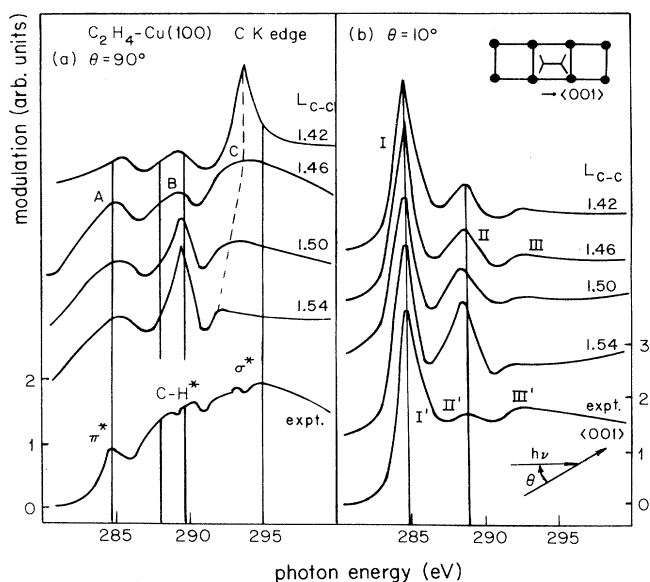


FIG. 2. Calculated C K-shell NEXAFS spectra of C_2H_4 -Cu(100) in the aligned-hollow model. The C—C bond length is changed from 1.42 to 1.54 Å. Incident x ray makes an angle θ with surface: (a) $\theta = 90^\circ$, (b) $\theta = 10^\circ$. The experimental spectra are quoted from Ref. 1.

reasonable to compare the above results with those of C_2H_4 -Pt(111) and C_2H_4 -Ag(100), in which L_{C-C} equals 1.49 and 1.40 Å, respectively.^{14,17} It is shown that the interaction between the C atom and Pt substrate is strongest in these substrates, while C-Ag interaction is weaker than the C-Cu and C-Pt interaction.

2. Carbon-hydrogen resonance in the C_2H_4 -Cu(100) system

We have determined the C—H bond length in a gas-phase ethylene molecule; it equals 1.09 Å. Now we investigate the C—H bond in the absorption system. We kept $L_{C-C} = 1.46$ Å and changed L_{C-H} from 1.00 to 1.15 Å. Figure 3 is a plot of the calculated NEXAFS spectra versus L_{C-H} . Figure 3(a) is the result for normal incidence, in which the C-H resonance shifts towards the lower energies when L_{C-H} increases. This rule is the same as that discussed above, and it confirms that peak B is closely related to the C—H bond. Figure 3(b) is the result for the grazing incidence, in which the first peak (labeled I) of the calculated spectra varies dramatically with L_{C-H} . It is obvious that the curves corresponding to $L_{C-H} = 1.15$ and 1.06 Å are not in agreement with the experiment, because the strength of peak I is too weak. As to the case of $L_{C-H} = 1.00$ Å, the position of peak I shifts towards higher energies; moreover, it is too weak to fit the experiment.

We turn to inspect the calculated curve corresponding to $L_{C-H} = 1.09$ Å, and find that this curve fits the experiment excellently. Therefore we can determine that the carbon-hydrogen bond length L_{C-H} equals 1.09 Å. For the ethylene molecule it does not change during chemisorption. This fact implies that the interaction between the hydrogen atom and the Cu substrate is weak.

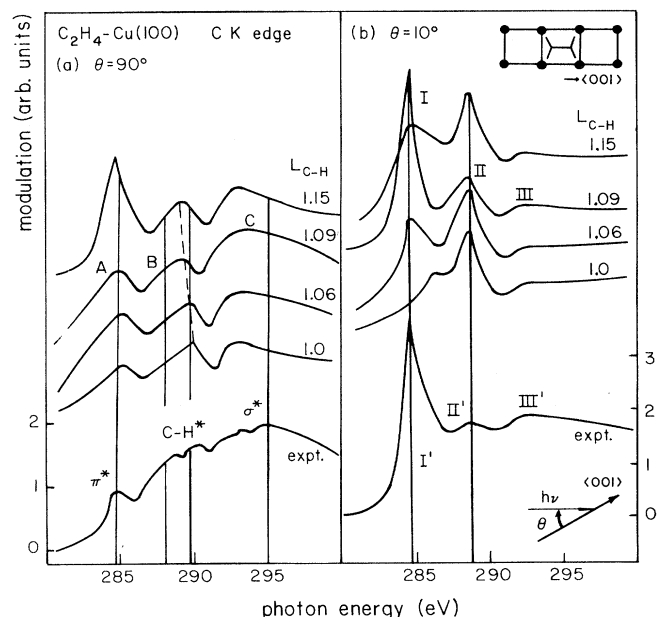


FIG. 3. Same as Fig. 2 except that the C—C bond length L_{C-C} is fixed, while the C—H bond length L_{C-H} is changed.

3. Determination of the H—C—H bond angle (α)

In order to determine the internal structure of the adsorbed ethylene molecule, we have to find the H—C—H bond angle α . Now we keep $L_{C-C}=1.46$ Å and $L_{C-H}=1.09$ Å, and change the angle α from 110 to 140°; the calculated C K-shell NEXAFS spectra have been plotted in Fig. 4. We find that these theoretical curves depend on α insensitively; they are similar to each other. By a detailed comparison we find a small difference existing in the case of normal incidence, i.e., the position of σ^* resonance shifts towards lower energies both for $\alpha < 130^\circ$ and $\alpha > 130^\circ$. Then we conclude that the H—C—H bond angle equals $(130^\circ \pm 5^\circ)$ which is larger than that in gas-phase ethylene molecules.

4. Determination of the adsorption distance L_{C-Cu}

The determination of the adsorption distance is very important for understanding the chemisorption process. It offers bonding information. We kept the structure constants of the ethylene molecule as determined above, but changed the adsorption height (h) from 1.1 to 1.4 Å, which is the distance of the C-C axis from the outmost layer of the Cu substrate as shown in the inset of Fig. 5(a). It is easy to see that the calculated curves are similar to each other, but we can find their small difference by a careful inspection. For grazing incidence the calculated curves, corresponding to $h=1.10, 1.20,$ and 1.40 Å, are not in agreement with experiment because the π^* resonance (peak I) is too weak. In contrast, the curves corresponding with $h=1.25, 1.30,$ and 1.35 Å agree with the experiment well. We conclude that $h=1.30 \pm 0.05$ Å, from which we can deduce that the L_{C-Cu} equals 1.90 ± 0.03 Å. This result agrees with the experimental result.^{1,2}

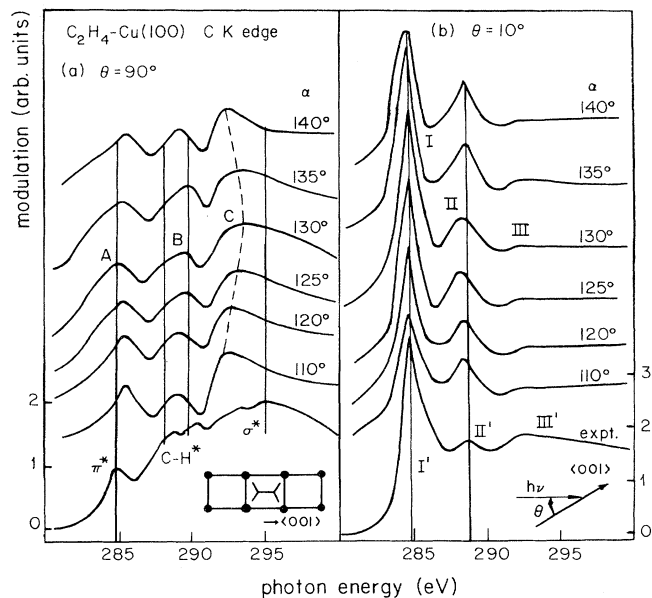


FIG. 4. Same as Fig. 2 except that the C—C bond length L_{C-C} is fixed, while the H—C—H bond angle α is changed.

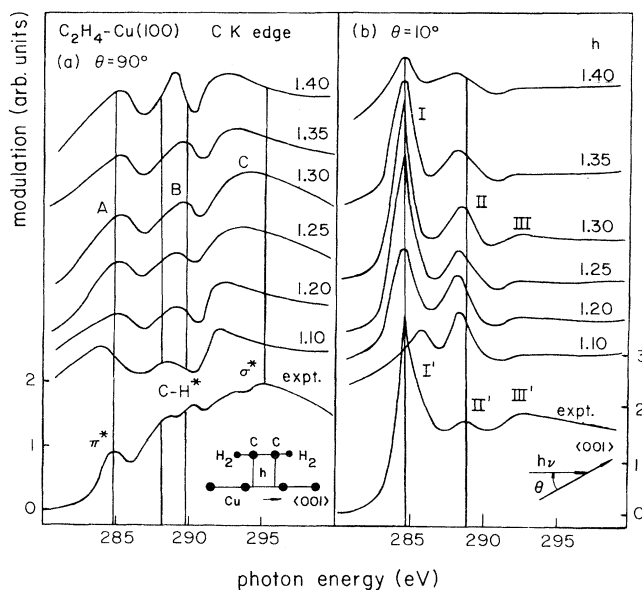


FIG. 5. Same as Fig. 2 except that the C—C bond length L_{C-C} is fixed, while the adsorption height (h) is changed.

C. R-factor analyses

To facilitate the comparison, R -factor analyses have been performed for four structural parameters. There are three kinds of R factors which are defined by Van Hove and Tong, Zanazzi and Jona, and by Pendry.¹⁸⁻²⁰ We define the average R factor as follows:

$$\bar{R}_i = \frac{1}{2}[\bar{R}_i(90^\circ) + \bar{R}_i(10^\circ)], \quad (20)$$

where $\bar{R}_i(90^\circ)$ and $\bar{R}_i(10^\circ)$ are R factors for normal and grazing incidence, respectively. The R factors are calcu-

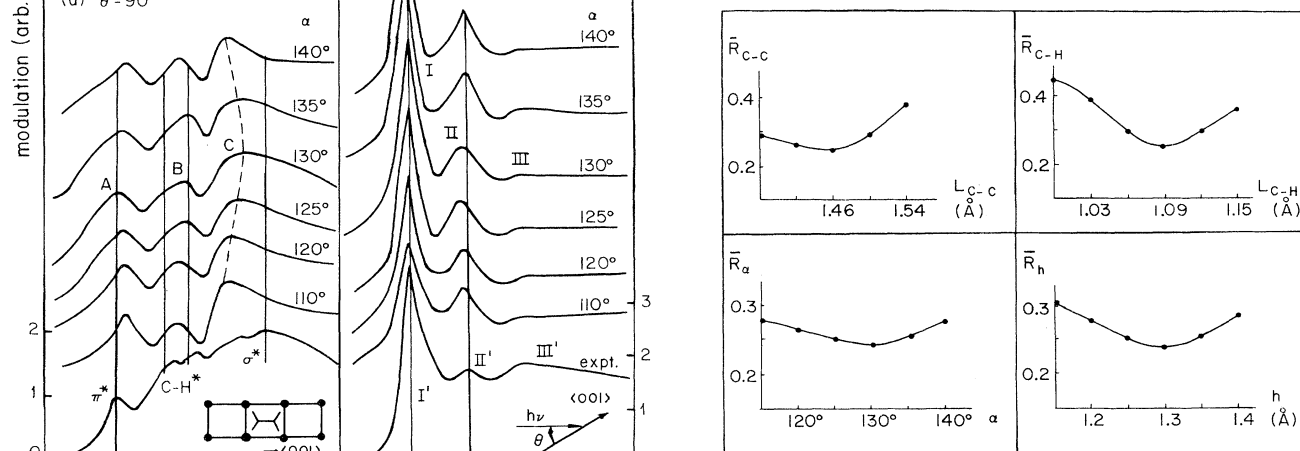


FIG. 6 Plot of the averaged R factors vs four structural parameters, i.e., the intramolecular bond length (L_{C-C} and L_{C-H}), the H—C—H bond angle (α), and the adsorption height (h), respectively.

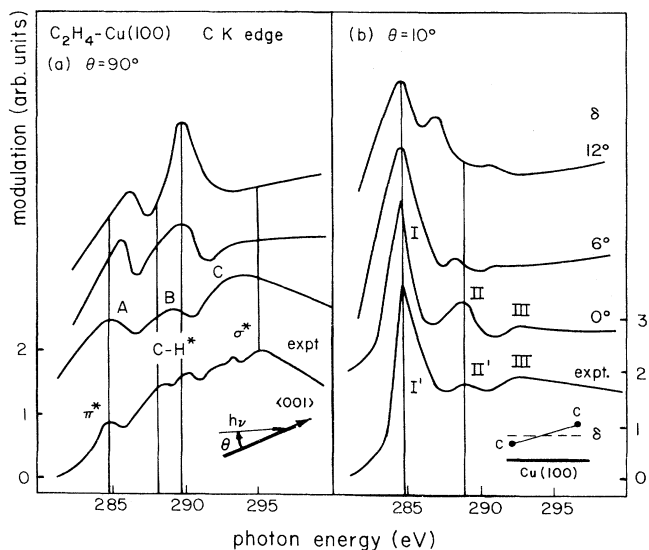


FIG. 7. Calculated C *K*-shell NEXAFS spectra of C_2H_4 -Cu(100) for the tilted model, in which the C—C bond makes an angle δ with Cu(100) surface. The experimental spectra are quoted from Ref. 1.

lated for the parameters L_{C-C} , L_{C-H} , α , and for h . The results have been plotted as a function of these structural quantities in Figs. 6(a)–6(d); the well-defined minima are seen at $L_{C-C}=1.46$ Å, $L_{C-H}=1.09$ Å, $\alpha=130^\circ$, and $h=1.3$ Å. It confirms that the results of the visual inspection are correct.

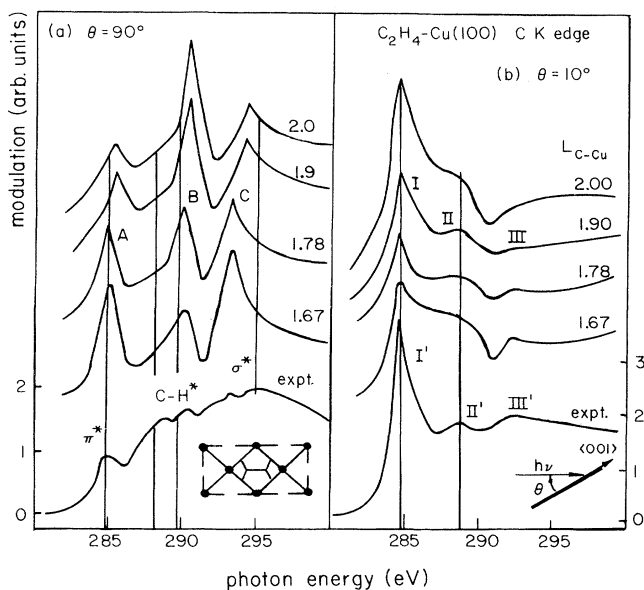


FIG. 8. Calculated C *K*-shell NEXAFS spectra of C_2H_4 -Cu(100) in the diagonal-hollow model. The values of adsorption distance are shown to be near by the related curves. Incident x-ray makes an angle θ with surface: (a) $\theta=90^\circ$, (b) $\theta=10^\circ$. The experimental spectra are quoted from Ref. 1.

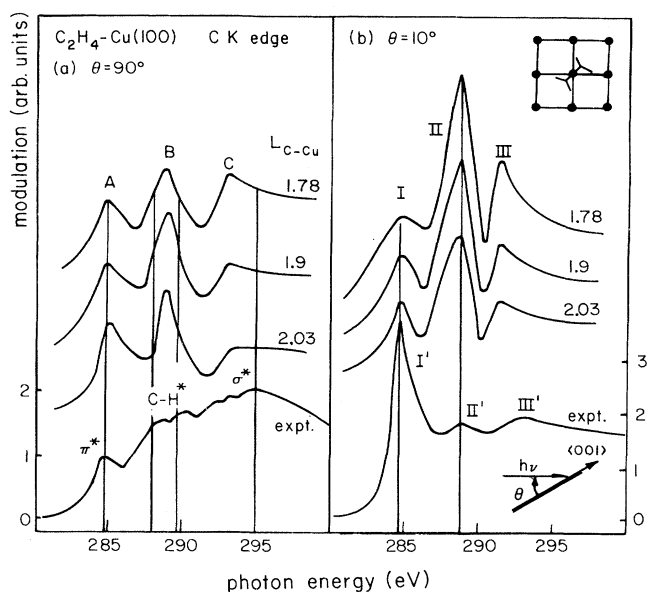


FIG. 9. Same as Fig. 8 except the calculation is performed with a diagonal-atop model.

D. Does the C-C axis tilt to the substrate?

Angle-dependent NEXAFS measurements demonstrated that the ethylene molecules were found to be lying flat on a Cu(100) surface.^{1,2} In order to identify this result, we have constructed a different model in which the C-C axis made a finite angle (δ) to the surface. In the calculation δ is set to equal 0° , 6° , and 12° . The calculated C *K*-shell NEXAFS spectra have been plotted in Fig. 7. Obviously, the curve corresponding to $\delta=6^\circ$ is similar to that of $\delta=0^\circ$. When $\delta=12^\circ$, the difference between those

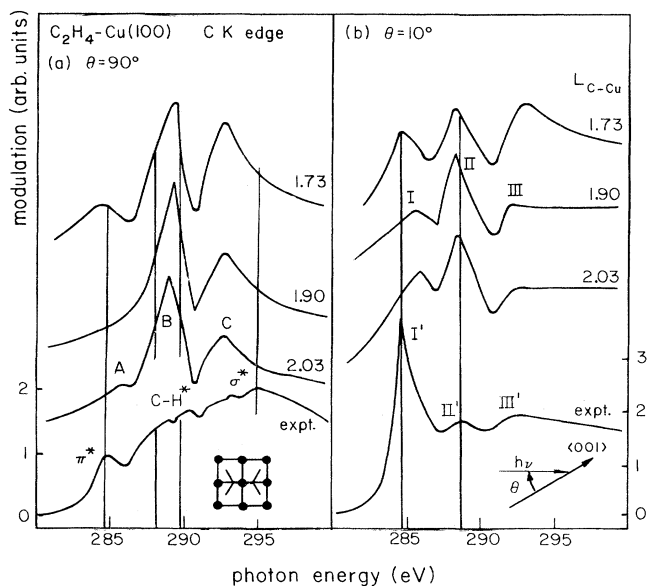


FIG. 10. Same as Fig. 8 except the calculation is performed with an aligned-atop model.

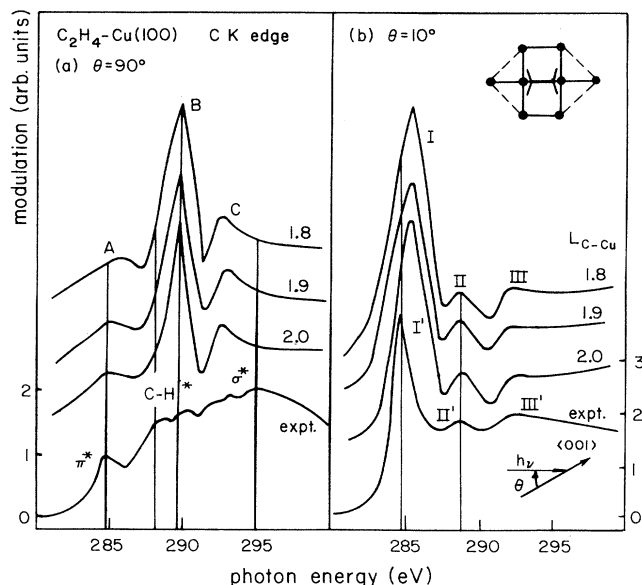


FIG. 11. Same as Fig. 8 except the calculation is performed with an aligned-bridge model.

curves is large; the positions of peak II and III shift towards lower energies. Moreover, in normal incidence the σ^* resonance coincides with C-H resonance. We conclude that the theoretical curve with $\delta=0^\circ$ is the best one to fit with the experimental spectrum, which indicates that the C-C axis is parallel to the Cu(100) surface.

E. Comparison between different structural models

The above-mentioned calculations are based on the aligned-hollow model. In order to determine the correct model we have to investigate other models. There are six possible highly symmetrical models for the C_2H_4 -Cu(100) system. We have calculated the C *K*-shell NEXAFS spectra for every model, and plotted the results in Figs. 8–12.

Figure 8 is the calculated C *K*-shell NEXAFS spectra for the diagonal-hollow model. In the calculation, the bond-length L_{C-Cu} was changed from 1.67 to 2.0 Å. For grazing incidence we found that the strength of C-C π^* resonance in the curves corresponding to $L_{C-Cu}=1.67$, 1.78, and 1.90 Å is too weak to fit with experiment. As for the curve corresponding to $L_{C-Cu}=2.0$ Å the third peak (labeled III in Fig. 8) disappears. These characters disagree with the experimental result; we have to rule out this model.

The calculation results for the diagonal-atop model have been plotted in Fig. 9. In grazing incidence the C-H resonance is too strong to agree with peak II in the experimental spectrum; this is a serious shortcoming. We also rule out this model.

As to the aligned-atop model, the theoretical curves were plotted in Fig. 10. For grazing incidence there is a

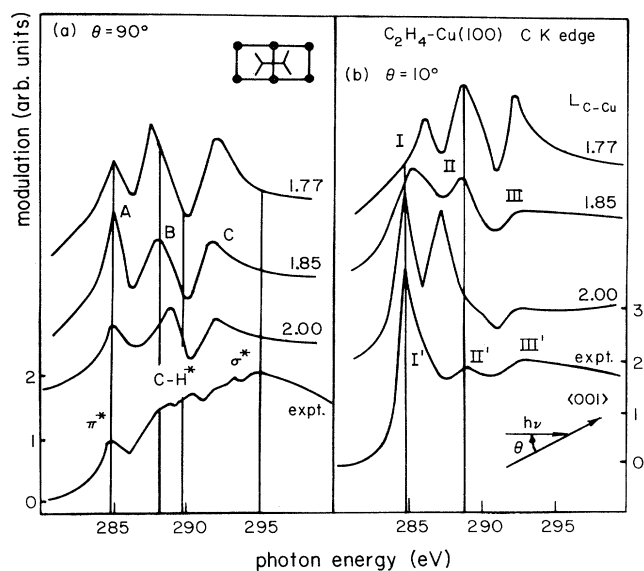


FIG. 12. Same as Fig. 8 except the calculation is performed with a perpendicular-bridge model.

serious shortcoming in the theoretical curves, i.e., the C-C π^* resonance is too weak to fit the experimental spectrum. So the aligned atop model is not correct.

We plotted the calculated C *K*-shell NEXAFS spectra for the aligned-bridge model in Fig. 11. The theoretical curves of grazing incidence agree with experiment very well; unfortunately, there is a very strong C-H resonance appearing for the normal incidence. We have to get rid of this model.

Figure 12 is the calculated results for the perpendicular-bridge model. It is easy to find that the calculated curves for grazing incidence disagree with experimental spectra. We also rule out this model.

IV. CONCLUSION

We have calculated the C *K*-shell NEXAFS spectra of the ethylene molecule as well as C_2H_4 adsorbed on the Cu(100) surface in terms of the MSC method. The result shows the following.

(a) C-H scattering resonance exists in C *K*-shell NEXAFS spectra either for a gas-phase ethylene molecule or for ethylene adsorbed on the Cu(100) surface.

(b) In C_2H_4 -Cu(100), the ethylene molecule is adsorbed in the hollow-site with the C—C bond parallel to the [001] or [010] direction.

(c) The C—C bond length is equal to 1.46 ± 0.04 Å; it is longer than the value in the gas phase. The elongation of L_{C-C} is due to the interaction between the adsorbate and the substrate atoms.

(d) The H—C—H bond angle is equal to $130^\circ \pm 5^\circ$,

which is larger than that in the gas-phase ethylene molecule by 10° .

(e) The C—Cu bond length equals $1.90 \pm 0.03 \text{ \AA}$.

From the above analyses we conclude that the MSC method is a useful technique for surface structure determination by NEXAFS.

ACKNOWLEDGMENTS

The co-authors at Zhejiang University are pleased to acknowledge the support of the National Natural Science Foundation of China and the Science Foundation of Zhejiang University.

-
- ¹D. Arvanitis, K. Baberschke, L. Wenzel, and U. Dobler, *Phys. Rev. Lett.* **57**, 3175 (1986).
- ²D. Arvanitis, U. Dober, L. Wenzel, K. Baberschke, and J. Stohr, *Surf. Sci.* **178**, 686 (1986).
- ³J. Stohr, D. A. Outka, K. Baberschke, D. Arvanitis, and J. A. Horsley, *Phys. Rev. B* **36**, 2976 (1987).
- ⁴J. A. Horsley, J. Stohr, and R. J. Koestner, *J. Chem. Phys.* **83**, 3146 (1985).
- ⁵P. J. Durham, J. B. Pendry, and C. H. Hodges, *Comput. Phys. Commun.* **25**, 193 (1982).
- ⁶J. B. Pendry, In *The Structure of Surface*, edited by M. A. Van Hove and S. Y. Tong (Springer-Verlag, Berlin, 1984).
- ⁷F. Sette, J. Stohr, and A. P. Hitchcock, *Chem. Phys. Lett.* **110**, 519 (1984); *J. Chem. Phys.* **81**, 4906 (1984).
- ⁸D. A. Outka, R. J. Maxdix, and J. Stohr, *Surf. Sci.* **164**, 235 (1985).
- ⁹S. Y. Tong and C. H. Li, in *Critical Reviews in Solid State and Materials Science* (CRC, Cleveland, 1981).
- ¹⁰C. H. Li, A. R. Lubinsky, and S. Y. Tong, *Phys. Rev. B* **17**, 3128 (1978).
- ¹¹T. Fujikawa, *J. Phys. Soc. Jpn.* **50**, 1321 (1981).
- ¹²J. C. Tang, in *The Structure of Surfaces II*, edited by J. F. Van der Veen and M. A. Van Hove (Springer-Verlag, Berlin, 1988).
- ¹³A. P. Hitchcock and C. E. Brion, *J. Electron Spectrosc. Relat. Phenom.* **10**, 317 (1977).
- ¹⁴J. Stohr, F. Sette, and A. L. Johnson, *Phys. Rev. Lett.* **53**, 1684 (1984).
- ¹⁵J. C. Tang, Y. B. Xu, and T. Fujikawa, *Vacuum* **42**, 499 (1991).
- ¹⁶*Comprehensive Organometallic Chemistry*, edited by G. Wilkinson (Pergamon, New York, 1982), Vol. 2.
- ¹⁷J. C. Tang, J. F. Shen, and Y. B. Chen, *Surf. Sci.* **244**, L125 (1991).
- ¹⁸M. A. Van Hove, S. Y. Tong, and M. H. Elconion, *Surf. Sci.* **64**, 65 (1977).
- ¹⁹E. Zanazzi and F. Jona, *Surf. Sci.* **62**, 61 (1977).
- ²⁰J. B. Pendry, *J. Phys. C* **13**, 937 (1980).